JOURNAL OF FINANCIAL AND QUANTITATIVE ANALYSIS VOL. 40, NO. 3, SEPTEMBER 2005
COPYRIGHT 2005, SCHOOL OF BUSINESS ADMINISTRATION, UNIVERSITY OF WASHINGTON, SEATTLE, WA 98195

https://doi.org/10.1017/S0022109000001915 Published online by Cambridge University Press

Pricing European and American Derivatives under a Jump-Diffusion Process: A Bivariate Tree Approach

Jimmy E. Hilliard and Adam Schwartz*

Abstract

We develop a straightforward procedure to price derivatives by a bivariate tree when the underlying process is a jump-diffusion. Probabilities and jump sizes are derived by matching higher order moments or cumulants. We give comparisons with other published results along with convergence proofs and estimates of the order of convergence. The bivariate tree approach is particularly useful for pricing long-term American options and long-term real options because of its robustness and flexibility. We illustrate the pedagogy in an application involving a long-term investment project.

I. Introduction

Merton (1976) developed the European option pricing model based on an underlying jump-diffusion process. Since then, Merton's model has been further refined and empirically tested in a number of applications. Papers in the mainstream finance literature include Ball and Torous (1985), Jorion (1988), Naik and Lee (1990), Bates (1991), (1996), Bakshi, Cao, and Chen (1997), Bakshi and Chen (1997), and Das and Sundaram (1999). The model generally performs better than a pure diffusion, in part because a jump-diffusion has higher moments that matter. Thus, more diverse distributions can be modeled with the process. Importantly, skewness and kurtosis are not fixed in this model.

Under the usual assumptions, the European jump-diffusion option pricing model admits to an easy solution that is the infinite sum of Black-Scholes (1973)-like expressions weighted by the corresponding probability of jump events. Convergence of the series typically depends only on the evaluation of a few terms, especially if these terms are centered around the expected number of jumps (see Bates (1991)). Double jump models such as those of Duffie, Pan, and Singleton (2000) incorporate jumps in volatility and in the underlying. However, we do not

*Hilliard, hilliar@lsu.edu, Louisiana State University, College of Business Administration, CEBA 2163, Baton Rouge, LA 70803; Schwartz, aschwartz@bus.olemiss.edu, University of Mississippi, School of Business Administration, 320 Holman Hall, University, MS 38677. We acknowledge the insights and helpful comments of Charles Cao (the referee) and Paul Malatesta (the editor). We assume full responsibility for all errors. Schwartz received research support from the office of Naval Research, Grant No. N000140310621.

address these models since they appear to be largely intractable in the context of derivatives with early exercise value. As Section IV and Table 2 demonstrate, the early exercise feature can add non-trivial value for long-term options.

Pricing American options under the assumption of an underlying jump-diffusion is problematic. Approaches in the literature include those of Amin (1993) and Bates (1991). Briefly, Amin constructs the binomial tree for the smooth component with corresponding risk-neutral probabilities. He then allows a jump to these same nodes (except jumps to adjacent nodes are not permitted) and finds the corresponding probability mass by centering it around these nodes. Amin notes that the discrete process converges weakly to the continuous-time jump-diffusions under mild regularity assumptions. Kushner and DiMasi (1978) also show that if a sequence of processes converge to their continuous-time limit American option prices with bounded payoffs also converge. Bates derives American prices by adjusting the European price with a correction similar to that developed by MacMillan (1987) and extended by Barone-Adesi and Whaley (1987).

The approach we take here is to model the jump-diffusion process using a bivariate tree. One factor is a discrete-time version of the smooth component. The second factor is a discrete-time version of log-normal jumps under Poisson compounding. We choose jump sizes and probabilities so that the discrete-time process converges to the local moments of the continuous-time jump-diffusion. The algorithm is simple and has excellent convergence properties. We prove weak convergence for fixed jump size and, in general, non-local convergence of all cumulants of finite order.

The importance of a bivariate tree formulation extends beyond the pricing of options with early exercise value. In fact, the bivariate tree can be used to price non-path-dependent complex functions of the underlying by evaluating the payoff and continuation values at all points on the grid. This feature makes it attractive for pricing real options with conditional decision features. The flexibility to price arbitrary payoff functions is an important point of departure from the models of Barone-Adesi and Whaley (1987) and Bates (1991), which adjust European prices by adding early exercise premiums specific to calls and puts. Amin's (1993) model, like the bivariate tree, can be used to price real options; however, simulations in Section IV demonstrate that the Amin model is not as robust as the bivariate tree.

Section II briefly reviews the jump-diffusion process and develops the jump sizes and probabilities for the bivariate tree. Section III investigates convergence properties. Section IV compares the results of the model with others published in the literature and Section V develops a real options example. Section VI concludes.

II. The Jump-Diffusion Process

Merton (1976) assumes that jump risk is unsystematic and forms a portfolio that yields the local risk-free return. Along with other standard assumptions, this allows him to develop the fundamental partial differential equation for pricing options. Bates (1991) uses an equilibrium model to develop the same functional form without the necessity of assuming an unsystematic jump component. Using

https://doi.org/10.1017/S0022109000001915 Published online by Cambridge University Press

Bates notation, the risk-neutralized version of the underlying jump-diffusion on the spot is

$$\frac{dS}{S} = (r - d - \lambda\bar{k})dt + \sigma dz + kdq, \tag{1}$$

where r is the risk-free rate, d is the continuous dividend yield, and σ is the volatility of the smooth diffusion component. The random variable dz is a standard Brownian motion and k is the random jump magnitude; $\log_e(1+k) \sim N(\gamma', \delta^2)$ where $\gamma' = \gamma - 0.5\delta^2$ and $E(k) \equiv \bar{k} = e^{\gamma} - 1$. A jump event occurs if and only if $dq = 1$. Otherwise $dq = 0$. The number of jump events is Poisson with intensity parameter λ. Equation (1) has the solution,

$$S_t = S_0 e^{(b-\lambda\bar{k}-\frac{\sigma^2}{2})t+\sigma z(t)} Y(n), \tag{2}$$

where $Y(n) = \Pi_{i=0}^{n(t)}(1+k_i)$, $k_0 = 0$, $n(t)$ is Poisson with parameter λ and $b \equiv r - d$ is the cost-of-carry. The assumptions of Merton (1976) or the setup of Bates (1991) give the fundamental partial differential and thus the price of the derivative.

A. The Bivariate Tree

A bivariate grid is constructed for the smooth diffusion and for log-normal jumps under Poisson compounding. The smooth diffusion jumps either up or down as in the standard univariate grid. However, the grid in the second factor consists of the Poisson-related jump components. Depending on accuracy and step size trade-offs, this factor may be represented by jumps to two up to any finite number of grid points. The two-node representation is appropriate when jump size is fixed. At least three nodes are required if the jump component is random. However, the three-node grid is generally not adequate since it matches only the first two moments. The five-, seven-, and nine-node grids are extremely accurate for the applications tested. These grids match, respectively, the first four, six, and eight local moments. Typically, the Poisson-related jump components map onto an odd number of points since the middle point corresponds to "no jump" and the remaining nodes are symmetric about the current level of the state variable. In the case of negative or positive skewness, an even-node grid can be effectively used, e.g., negative skewness can be induced by a four-node grid with two down jumps, no jump, and a positive jump. However, non-normal skewness can also be induced for a symmetric set of nodes by choice of probabilities.

B. The Grid

Rewrite equation (2) as

$$V_t \equiv \ln\left(\frac{S_t}{S_0}\right) \equiv X_t + Y_t, \tag{3}$$

where

$$X_t \equiv \left(b - \lambda\bar{k} - \frac{\sigma^2}{2}\right)t + \sigma z(t),$$

https://doi.org/10.1017/S0022109000001915 Published online by Cambridge University Press

is arithmetic Brownian motion and

$$Y_t \equiv \sum_{i=0}^{n(t)} \ln(1+k_i) \tag{4}$$

is normal under Poisson compounding. Motivated by this decomposition, define the $2 \times (2m+1)$ bivariate grid as

$$V_{i+1}^{+} = V_i + \sigma\sqrt{\Delta} + jh, \quad j = 0, \pm 1, \pm 2, \ldots, \pm m, \tag{5}$$

$$V_{i+1}^{-} = V_i - \sigma\sqrt{\Delta} + jh, \quad j = 0, \pm 1, \pm 2, \ldots, \pm m, \tag{6}$$

where $i = 0, 1, \ldots, n$ is the time index, Δ is the length of the time step, $2\sigma\sqrt{\Delta}$ is the distance between node points for the smooth factor, and h is the distance between node points for the compound jump factor. For a derivative $F = F(V,t)$, the one-period recursion relation is

$$F(V_i,t) = \frac{\sum_{j=-m}^{m}\left[pq(j)F(V_i+\sigma\sqrt{\Delta}+jh,t+\Delta)+(1-p)q(j)F(V_i-\sigma\sqrt{\Delta}+jh,t+\Delta)\right]}{(1+r\Delta)}, \tag{7}$$

where $q(j) \equiv q_{m+j+1}$. Joint probabilities are of the form pq because of the assumed independence between jump and smooth factors.

The grid in the X_t dimension is the Cox, Ross, and Rubenstein (1979) binomial as transformed by Nelson and Ramaswamy (1990) to give constant volatility. Jumps in the smooth diffusion are of magnitude $X_{i+1} - X_i = \pm\sigma\sqrt{\Delta}$ with up jump probability,

$$p = 0.5\left(1 + \frac{\sqrt{\Delta}}{\sigma}\left(b - \lambda\bar{k} - \frac{\sigma^2}{2}\right)\right). \tag{8}$$

The grid in the Y dimension is determined by jh, where h is the distance between nodes and j is the number of jumps up or down on either side of the central node. For a $2m+1 \equiv$ "M-node" grid, the probabilities $q_j, j = 1, 2, \ldots, M$ are chosen to match the first $2m$ local moments of the continuous-time distribution of Y. For a symmetric tree, this means

$$\sum_{j=-m}^{m} (jh)^{i-1} q(j) = \mu'_{i-1} \equiv E[Y_\Delta]^{i-1} \equiv E\left[\sum_{j=0}^{n(\Delta)} \ln(1+k_j)\right]^{i-1}, \quad i = 1, 2, \ldots, M, \tag{9}$$

where μ'_i is the ith local moment of Y and $i = 1$ corresponds to the additional condition that $\sum q_j = \mu'_0 = 1$. For example, the probabilities must satisfy the

https://doi.org/10.1017/S0022109000001915 Published online by Cambridge University Press

matrix equations $Aq = \mu^*$ where μ^* is the mean vector with element i divided by h^{i-1}. For a five-node tree, the equations are

$$\text{(10)} \qquad \begin{pmatrix} 1 & 1 & 1 & 1 & 1 \\ -2 & -1 & 0 & 1 & 2 \\ 4 & 1 & 0 & 1 & 4 \\ -8 & -1 & 0 & 1 & 8 \\ 16 & 1 & 0 & 1 & 16 \end{pmatrix} \begin{pmatrix} q_1 \\ q_2 \\ q_3 \\ q_4 \\ q_5 \end{pmatrix} = \begin{pmatrix} 1 \\ \frac{\mu_1'}{h} \\ \frac{\mu_2'}{h^2} \\ \frac{\mu_3'}{h^3} \\ \frac{\mu_4'}{h^4} \end{pmatrix},$$

$$\text{(11)} \qquad \begin{pmatrix} q_1 \\ q_2 \\ q_3 \\ q_4 \\ q_5 \end{pmatrix} = \frac{1}{24} \begin{pmatrix} 0 & 2 & -1 & -2 & 1 \\ 0 & -16 & 16 & 4 & -4 \\ 24 & 0 & -30 & 0 & 6 \\ 0 & 16 & 16 & -4 & -4 \\ 0 & -2 & -1 & 2 & 1 \end{pmatrix} \begin{pmatrix} 1 \\ \frac{\mu_1'}{h} \\ \frac{\mu_2'}{h^2} \\ \frac{\mu_3'}{h^3} \\ \frac{\mu_4'}{h^4} \end{pmatrix}.$$

The moment matrix, A, is a special case of the Vandermonde matrix and is easily inverted in exact form (Appendix A). The system can be implemented by expressing moments as a function of cumulants. However, for sufficiently fine grids the approximation $\mu' \approx \kappa_i$ is accurate since $\mu_1' = \kappa_1$ and $\mu_i' = \kappa_i + O(\Delta^2)$, $i = 2, 3, \ldots$ (Stuart and Ord (1994)). Cumulants as a function of jump-diffusion parameters are given in Appendix B. The five-node version requires the first four cumulants, the seven-node version the first six cumulants, and so on.

Node spacing is computed according to

$$\text{(12)} \qquad h = \alpha\sqrt{(\gamma')^2 + \delta^2}.$$

The functional form of h follows from weak convergence and a local moment-matching condition. Specifically, h as in equation (12) and $\alpha = 1$ yield weak convergence for the special case of fixed jump sizes. In addition, if the middle node probability is set to $1 - \lambda\Delta$, local moment matching for the three-node tree requires that $\alpha = 1$. If more than three nodes are used, the no-jump node will not have probability $1 - \lambda\Delta$. Using ordinary least squares to minimize deviations and dropping higher order terms results in h as in equation (12) with $0 < \alpha < 1$. Our simulations use $\alpha = 1$ because it is empirically determined to give better accuracy.[1]

III. Convergence of the Discrete Process

Weak convergence of the discrete-price process to its continuous-time limit is sufficient for convergence of European put and call prices (Nelson and Ramaswamy (1990)). We show conditions under which the discrete X_n and Y_n processes defined on the bivariate tree converge weakly to their continuous-time counterparts at an arbitrary but finite time $T \geq t_0$. Furthermore, by the independence of the X_n and Y_n processes and the continuous mapping theorem

[1] Fortran code for the bivariate binomial is available from the authors.

https://doi.org/10.1017/S0022109000001915 Published online by Cambridge University Press

$S_0 e^{V_n} = S_0 e^{X_n + Y_n}$ converges weakly to S_T. We address here only the convergence of the Y_n process since the weak convergence of X_n to X_T is a standard result in stochastic processes.

A. Weak Convergence of Y_n

Using jump independence and iterated expectations, the characteristic function of the continuous-time process Y_T is

$$\begin{aligned} (13) \quad \phi_{Y_T}(\theta) &= E\left(e^{i\theta\left(\sum_{i=0}^{n(T)} \ln(1+k_i)\right)}\right) \\ &= E_{n(T)}\left(\left[E\left(e^{i\theta(\ln(1+k)}\right)\right]^{n(T)} \middle| n(T)\right), \end{aligned}$$

$$(14) \quad \phi_{Y_T}(\theta) = \sum_{n=0}^{\infty}\left[\left(e^{i\theta\gamma' + \frac{\theta^2\delta^2}{2}}\right)^n e^{-\lambda T}\frac{(\lambda T)^n}{n!}\right] = e^{\lambda T\left(e^{i\theta\gamma' + \frac{\theta^2\delta^2}{2}} - 1\right)}.$$

The Y_n process converges weakly when the jump size is fixed, i.e., when $\delta = 0$. The two-node values are zero and $h = \gamma'$. The probability of a jump is $q_2 = \lambda\Delta = \lambda T/n$. Weak convergence of Y_n to Y_T follows because

$$\begin{aligned} (15) \quad \phi_{Y_n}(\theta) &= \left(1 - \frac{\lambda T}{n} + \frac{\lambda T}{n}e^{i\theta\gamma'}\right)^n \\ &= \left(1 + \frac{\lambda T}{n}\left(e^{i\theta\gamma'} - 1\right)\right)^n \quad \to \quad e^{\lambda T\left(e^{i\theta\gamma'} - 1\right)} = \phi_{Y_T}(\theta). \end{aligned}$$

B. Convergence of Cumulants

Local matching of moments is sufficient for the matching of cumulants at arbitrary time T. Specifically, we show that matching the first $2m$ local moments (to $O(\Delta^2)$) to the moments of the continuous-time process implies that the first $2m$ cumulants of Y_n converge to those of Y_T. We concern ourselves only with Y_n since X_n converges weakly to X_T, a stronger condition.

Denote time-t dependence of moments and cumulants of the continuous-time X_t process by $\mu_j'(t)$ and $\kappa_j(t)$, respectively. To simplify notation, the argument is omitted when the time dependence is local ($t = \Delta$). From Appendix B, cumulants are linear homogeneous in t so that $n\kappa_j \equiv \kappa_j(T)$, $j = 1, 2, \ldots$. Expanding exponential terms and matching the first $2m$ local moments gives

$$\begin{aligned} (16) \quad \phi_{Y_n}(\theta) &= \left(1 + \sum_{j=1}^{2m+1} q_j\left(e^{i\theta(j-m-1)h} - 1\right)\right)^n \\ &= \left(1 + \sum_{j=1}^{2m}\mu_j'\frac{(i\theta)^j}{j!} + \varepsilon(i\theta)^{2m+1}\frac{\mu_{2m}}{2m!}\right)^n, \quad |\varepsilon| < 1, \end{aligned}$$

https://doi.org/10.1017/S0022109000001915 Published online by Cambridge University Press

where the form of the remainder term follows from a result in Stuart and Ord (1994). The cumulant function is

$$\Psi_{Y_n}(\theta) = n \ln \left(1 + \sum_{j=1}^{2m} \kappa_j \frac{(i\theta)^j}{j!} + \varepsilon (i\theta)^{2m+1} \frac{\kappa_{2m}}{2m!} + O(\Delta^2) \right), \tag{17}$$

but $\kappa_j = (1/n)\kappa_j(T)$ can be made arbitrarily small. Therefore, for some $n > n_0$,

$$\Psi_{Y_n}(\theta) = \sum_{j=1}^{2m} \kappa_j(T) \frac{(i\theta)^j}{j!} + \varepsilon (i\theta)^{2m+1} \frac{\kappa_{2m+1}(T)}{(2m+1)!} + O\left(\frac{1}{n^2}\right), \tag{18}$$

so that the first $2m$ cumulants of Y_n converge to those of Y_T.

In summary, matching local moments yields weak convergence when jump size is fixed. This is sufficient for the convergence of European option prices. In the more general case of log-normal jumps, matching the first $2m$ local moments results in matching the first $2m$ cumulants at arbitrary but finite time T. While this approximation may be accurate, it is not in general sufficient to guarantee convergence to continuous-time option prices.

C. Robustness

The bivariate algorithm converges quickly and accurately for cases in the literature. However, convergence problems are not unlike those in the binomial algorithm for a smooth diffusion. For example, the smooth diffusion algorithm may require special jump conventions in order to preserve legitimate probabilities under transformations required for recombining trees. These conditions are investigated extensively in Nelson and Ramaswamy (1990). Likewise, the M-node tree can produce negative probabilities and convergence problems for certain parameter sets.

Jump probabilities for all versions of M-node are on [0,1] when γ', the average jump size, is zero. A small step size is required to insure that the middle node probability is positive but this is always possible by choosing a sufficiently large number of steps. The probability vectors for five-, seven-, and nine-node when $\gamma' = 0$ are:

$$\begin{aligned}
\mathbf{q}_5^T &= \left(\tfrac{1}{12}\lambda\Delta \;\; \tfrac{1}{6}\lambda\Delta \;\; 1 - \tfrac{1}{2}\lambda\Delta \;\; \tfrac{1}{6}\lambda\Delta \;\; \tfrac{1}{12}\lambda\Delta \right) \\
\mathbf{q}_7^T &= \left(\tfrac{1}{180}\lambda\Delta \;\; \tfrac{1}{20}\lambda\Delta \;\; \tfrac{1}{4}\lambda\Delta \;\; 1 - \tfrac{11}{18}\lambda\Delta \;\; \tfrac{1}{4}\lambda\Delta \;\; \tfrac{1}{20}\lambda\Delta \;\; \tfrac{1}{180}\lambda\Delta \right) \\
\mathbf{q}_9^T &= \left(\tfrac{1}{6720}\lambda\Delta \;\; \tfrac{11}{2520}\lambda\Delta \;\; \tfrac{13}{240}\lambda\Delta \;\; \tfrac{29}{120}\lambda\Delta \;\; 1 \right. \\
&\quad \left. - \tfrac{173}{288}\lambda\Delta \;\; \tfrac{29}{120}\lambda\Delta \;\; \tfrac{13}{240}\lambda\Delta \;\; \tfrac{11}{2520}\lambda\Delta \;\; \tfrac{1}{6720}\lambda\Delta \right).
\end{aligned}$$

The more complex analysis of probabilities when γ' is nonzero is simplified by noting that h^i and κ_i are homogeneous of order i in δ and γ'. Thus, the right-hand side of the moment-matching equations is linear homogeneous of order 0 (Appendix B). Since the inverse of the moment matrix consists of constants, the jump probabilities are also linear homogeneous of order 0. This means that

$$q(\lambda t, \delta, \gamma') = q(\lambda t, \beta, 1), \tag{19}$$

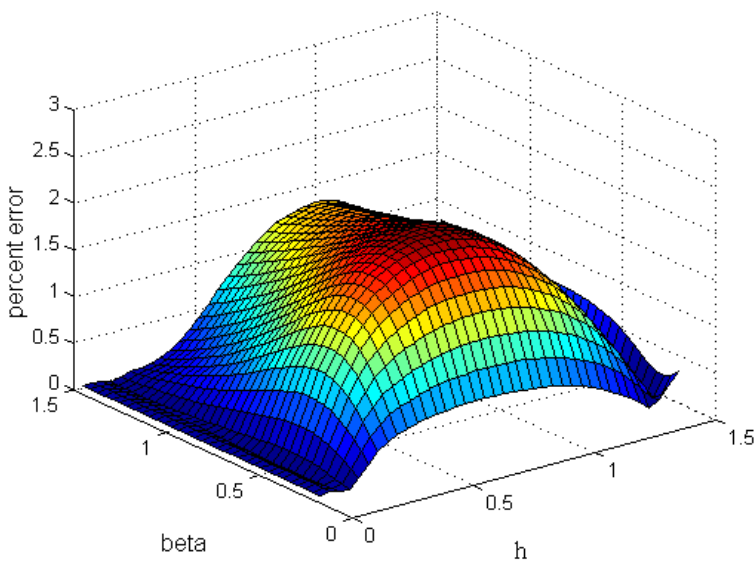
https://doi.org/10.1017/S0022109000001915 Published online by Cambridge University Press

where $\beta \equiv \delta/\gamma'$.[2] This property reduces dimensionality by one and holds for all versions of *M*-node.

A surface of percent errors as a function of *h* and β is shown in Figure 1. The surface was generated using 400 steps and the seven-node algorithm. The options are at-the-money European calls on futures contracts with fixed parameters $\sigma = 0.20$, $\lambda = 1$, $T = 0.25$, and strike =250. Errors are generally much less than 1% for all *h* and β. Errors approach zero for all values of β near zero, corresponding to $\delta = 0$ (fixed jump sizes). Extensive simulations with five-node proved to be somewhat less accurate than seven-node. However, simulations with nine-node revealed no incremental improvement in accuracy.

FIGURE 1

Pricing Error vs. *h* and Beta: Calls on Futures



The benchmark is Merton's model. Parameters are $\lambda = 1$, $\sigma = 0.10$, $r = 0.10$, and $\beta \equiv \delta/\gamma'$ and $h = \sqrt{\gamma'^2 + \delta^2}$. At-the-money underlying = \$250. Seven-node tree with 400 steps.

Plots of absolute errors vs. the number of steps quantify the order of convergence. Similar to the CRR binomial, the bivariate binomial exhibits order one convergence (see Figure 2). Details of the convergence measure are given in Appendix C.

IV. Simulations

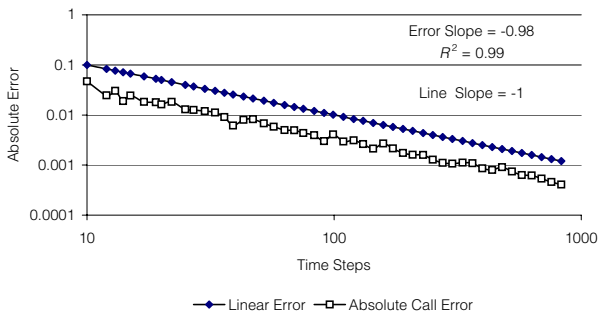
The accuracy of the approximation is evaluated in several ways. First, American call prices on futures are computed using the same parameters as those used

[2]Note that δ/γ' is the coefficient of variation of $\ln(1 + k)$.

https://doi.org/10.1017/S0022109000001915 Published online by Cambridge University Press

FIGURE 2

Order of Convergence: In-the-Money Call on Futures



Parameters are $\sigma = 0.20$, $\lambda = 10$, $\gamma = 0.01$, $\delta = 0.03$, $r = 0.10$, and $T = 0.25$. Underlying = \$250 and strike = \$235. Seven-node tree.

by Bates (1991). Next, both European and American call prices are computed using the parameters of Amin (1993). In these simulations, the moment-matching model produces results that are economically equal to or better than those of competing models. The model is markedly superior in cases where conditional jump volatility (δ) is high relative to smooth diffusion volatility (σ).

A. Empirical Comparisons

American call prices on futures are generated by the seven-node model and compared to those of Bates (1991). The Bates prices are generated by i) a modified version of the MacMillan (1987) quadratic approximation method and ii) "... by the binomial option pricing methodology for the diffusion part, augmented by probability-weighted numerical integration for jump-contingent expected values" Bates (1991), p. 1029. We find that seven-node prices, the Bates-MacMillan prices, and finite difference prices are economically identical.[3] For call prices ranging from \$0.35 to \$30, the seven-node algorithm with 100 steps differed from the finite difference algorithm by no more than \$0.01 or less than ½%. The performance of the Bates-MacMillan analytic approximation is similar.

Table 1 depicts simulations of both European and American put options on the spot. In this table, seven-node prices are compared with those of Amin (1993). Amin's algorithm is based on the binomial tree where jumps to adjacent nodes represent the smooth diffusion and jumps to nodes outside the middle three represent the Poisson jump components. Amin chooses a rectangular grid with the number of states equal to twice the number of steps+1 ($m = 2n$ steps+1). Relative to the center state, the maximum and minimum nodes are therefore n-nodes away. For each state, the probability distribution is centered at that node value and the probability mass surrounding the remaining nodes is computed numerically.

[3]No table is shown since price differences are consistently zero or one cent.

https://doi.org/10.1017/S0022109000001915 Published online by Cambridge University Press

The distribution is truncated at the closer of the region outside $\pm 3\delta$, the boundary nodes, or *n*-nodes away. Options at boundary nodes are set equal to intrinsic values or European values.

TABLE 1

European and American Put Prices on the Spot

	European Puts			Percent Errors		American Puts	
Strike	Merton	7-Node	Amin	7-Node	Amin	7-Node	Amin
Panel A. $\lambda = 5$, $\gamma = 0$, $\delta = \sqrt{0.05}$, *and* $\sigma = \sqrt{0.05}$ *(equal jump and smooth volatility)*							
30	2.621	2.621	2.623	0.033	0.071	2.718	2.720
35	4.412	4.414	4.415	0.054	0.077	4.603	4.603
40	6.696	6.698	6.701	0.031	0.075	7.028	7.030
45	9.422	9.427	9.426	0.051	0.040	9.954	9.954
50	12.524	12.526	12.528	0.017	0.033	13.316	13.318
Panel B. $\lambda = 5$, $\gamma = 0$, $\delta = 0.3$, *and* $\sigma = 0.10$ *(large relative jump volatility)*							
30	3.918	3.915	3.894	−0.088	−0.634	4.043	4.042
35	5.982	5.993	5.972	0.184	−0.167	6.199	6.202
40	8.458	8.465	8.461	−0.085	0.043	8.788	8.805
45	11.302	11.299	11.318	−0.026	0.140	11.785	11.812
50	14.460	14.483	14.487	0.157	0.188	15.162	15.172
Panel C. $\lambda = 5$, $\gamma = 0$, $\delta = \sqrt{0.05}$, *and* $\sigma = 0.05$ *(larger relative jump volatility)*							
30	2.172	2.189	1.837	0.781	−15.444	2.272	2.057
35	3.810	3.788	3.553	−0.580	−6.738	3.965	3.878
40	5.980	6.004	5.783	0.401	−3.291	6.313	6.249
45	8.650	8.638	8.501	−0.143	−1.730	9.165	9.157
50	11.756	11.787	11.646	0.267	−0.936	12.566	12.559

Merton's (1976) model is the benchmark for European puts. Amin is the tree algorithm developed by Amin (1993). Bivariate uses the (two) × seven-node tree. Both the seven-node and Amin approximations are implemented with 200 steps. The underlying spot is $40 and pays no dividends. The risk-free rate is 8% and the time-to-maturity is one year. Relative jump volatility is defined as δ/σ.

The Merton model is used as the benchmark for the European put prices. Both the seven-node and Amin approximations perform well in Table 1, Panel A, where conditional jump volatility ($\delta = \sigma = \sqrt{0.05}$) is equal to smooth volatility. When compared to Merton, each algorithm has errors that are economically insignificant (seven-node error is less than 0.06% and Amin error less than 0.08%). The algorithms perform well (Panel B) but with slight degradation when conditional jump volatility is relatively large compared to smooth volatility ($\delta = 0.3$ and $\sigma = 0.10$). The largest errors are 0.157% (seven-node) and 0.188% (Amin). A more extreme case is found in Panel C, where conditional jump volatility is much larger than smooth volatility ($\delta = \sqrt{0.05}$ and $\sigma = 0.05$). Seven-node errors are still small with maximum error less than 0.80%. The Amin algorithm has errors ranging from a minimum of about 1% to a maximum of over 15%.

Differences in the Amin and seven-node tree are similar for American options, i.e., the values are less than 0.23% in Panels A and B of Table 1 but differences in Panel C exceed 10% for the deep-in-the-money put. Unlike the case for European options, American options have no generally accepted benchmark.

The state space in Amin's algorithm is a function of drift, smooth sigma, and the number of steps. Jump volatility, mean jump size, and intensity are imbedded in the risk-neutralized probabilities. The state space itself is invariant of these parameters. In particular, large conditional jump volatility (δ) results in a truncated distribution that is nonzero outside the state space. This can be remedied some-

https://doi.org/10.1017/S0022109000001915 Published online by Cambridge University Press

what by expanding the number of steps and thus the state space. However, this remedy fails as σ approaches zero since in this case the Amin state space reduces to the deterministic drift component. In contrast, the bivariate tree accommodates a more general jump-diffusion since the state space is a function of σ, δ, and γ.

Extensive simulations indicate that both the bivariate and Amin algorithms perform well when conditional jump volatility is small relative to smooth volatility. However, the Amin algorithm degrades quickly when δ is larger than σ. Relatively large δs can be expected for commodities, some currencies, and real options. Conversely, one expects that σ should be larger for equities and especially for equity indices. The evidence is mixed. Recent studies obtain parameter estimates using the stochastic volatility model with jumps (SVJ) and other extensions that nest the jump-diffusion (JD) model. As a rough approximation, we use reported estimates of mean long-term volatility $\equiv \sqrt{\theta}$ as a proxy for σ in the JD model. Eraker (2004) in an SVJ model finds parameter estimates $(\sqrt{\theta}, \delta) = (0.2040, 0.0663)$ for the S&P index. Similarly, using an SVJ model and the S&P index, Pan (2002) finds that conditional jump volatility is smaller $(\sqrt{\theta}, \delta) = (0.1237, 0.0387)$. However, from Bakshi and Cao (1997) and their findings on the S&P index, we calculate $(\sqrt{\theta}, \delta) = (0.1404, 0.2646)$ and from Bakshi and Cao (2004) we calculate $(\sqrt{\theta}, \delta) = (0.1363, 0.19)$ for a sample of 50 firms.[4]

B. The Early Exercise Premium

Early exercise value is an important part of American option value at longer maturities. While the majority of traded options have maturities of less than 60 days, long-term equity anticipation securities (LEAPS) can extend up to three years and real options can have lives exceeding 10 years. Table 2 gives results for the same parameters as those we use in Panel A of Table 1 except maturities are 60 days (Panel A), one year (Panel B), five years (Panel C), and 10 years (Panel D). Note that in Panel A, column seven, the early exercise premium makes up less than 1% of American option value for these short-term options. The numbers for this example range from 46 to 86 basis points. However, at one, five, and 10 years the maximum early exercise premiums are 5.9%, 24.4%, and 43.8%, respectively.

C. Numerical Greeks

It is not possible to form a riskless hedge from the option and the underlying asset in the case of a jump-diffusion with random jump magnitude. However, as Merton (1976) notes, delta $(\partial F(S,t)/\partial S)$ can be computed in any case and used to hedge risk other than that caused by the jump. In Merton's setup, this means that the unsystematic jump risk is not hedged. In a Bates (1991) world, where the risk is priced by placing restrictions on technologies and preferences, the unhedged jump risk may be systematic.

Numerical deltas are calculated at time $n-1$ from values at time n. For a tree with M-nodes, the approximation is

[4]Differences in S&P index parameter estimates can be explained in part by different estimation techniques and data sets.

https://doi.org/10.1017/S0022109000001915 Published online by Cambridge University Press

TABLE 2

Early Exercise Premium

	European Puts			American Puts		
Strike	Merton	7-Node(E)	Error(%)	7-Node(A)	7-Node(CV)	Ex. Prem. (%)
Panel A. Maturity = 60 days						
30	0.411	0.407	−1.147	0.408	0.413	0.460
35	1.146	1.152	0.482	1.159	1.153	0.571
40	2.857	2.854	−0.094	2.871	2.874	0.598
45	6.097	6.104	0.118	6.144	6.137	0.658
50	10.281	10.277	−0.035	10.366	10.370	0.858
Panel B. Maturity = one year						
30	2.621	2.622	0.014	2.718	2.718	3.558
35	4.412	4.414	0.047	4.603	4.601	4.109
40	6.696	6.698	0.034	7.028	7.026	4.693
45	9.422	9.427	0.048	9.954	9.950	5.301
50	12.524	12.526	0.018	13.316	13.314	5.935
Panel C. Maturity = five years						
30	5.618	5.622	0.072	6.971	6.967	19.367
35	7.437	7.442	0.072	9.391	9.386	20.762
40	9.412	9.418	0.066	12.081	12.075	22.057
45	11.519	11.526	0.061	15.019	15.012	23.267
50	13.741	13.749	0.058	18.185	18.177	24.406
Panel D. Maturity = 10 years						
30	5.263	5.288	0.477	8.499	8.474	37.893
35	6.628	6.659	0.467	11.006	10.975	39.611
40	8.063	8.100	0.454	13.736	13.699	41.144
45	9.558	9.601	0.449	16.674	16.631	42.528
50	11.105	11.154	0.439	19.805	19.757	43.791

Merton's model is the benchmark for European puts. The spot price is $S = 40$ and parameters are $r = 0.08$, $\lambda = 5$, $\gamma = 0$, $\delta = \sqrt{0.05}$, and $\sigma = \sqrt{0.05}$. Control variates are used to improve 7-node accuracy. The early exercise premium (Ex. Prem. %) is defined as (7-node(CV)− Merton)/Merton∗100. 7-node implemented with 200 steps.

$$\frac{\partial}{\partial S}F(S,T) \approx q_1\frac{F\left(S_1^+,\Delta\right)-F\left(S_1^-,\Delta\right)}{S_1^+-S_1^-} + q_2\frac{F\left(S_2^+,\Delta\right)-F\left(S_2^-,\Delta\right)}{S_2^+-S_2^-}+\ldots + q_M\frac{F\left(S_M^+,\Delta\right)-F\left(S_M^-,\Delta\right)}{S_M^+-S_M^-}. \tag{20}$$

Subscripts denote node position in the jump dimension and superscripts $(\pm)$ denote an up or down node in the smooth diffusion. The second derivative, gamma $\equiv (\partial F^2(S,t)/\partial S^2)$, is computed by the same formula but node values one step forward are first partials, i.e., replace F by $\partial F/\partial S$ in equation (20).

Table 3 compares first and second partials for puts on the spot computed numerically by seven-node with 600 steps and by analytic partials using Merton's result. Parameters are given in the table. The four panels correspond to jump-diffusions with, respectively, jump volatility small relative to smooth volatility (δ/σ is small), equal jump and smooth volatility, large relative jump volatility, and still larger relative jump volatility. Compared to the Merton benchmark, the numerical partials in the first two panels are correct to the third decimal. The errors increase when jump volatility is large relative to smooth volatility. For the at-the-money strike in Panel C, the Merton delta is -0.3221, and the numerical

https://doi.org/10.1017/S0022109000001915 Published online by Cambridge University Press

delta is −0.3155. Corresponding numbers for gamma are 0.01464 and 0.01677. The delta approximation remains accurate in Panel D, but the numerical gamma has relatively large errors for the deep out-of-the-money put.

TABLE 3

Put Option Greeks: Jump-Diffusion Underlying

	Put Delta (Δ)				Put Gamma (Γ)			
Strike	Merton	7-Node(E)	7-Node(A)	Error(E)	Merton	7-Node(E)	7-Node(A)	Error(E)
Panel A. $\lambda = 0.0001$, $\gamma = 0$, $\delta = 0.0001$, *and* $\sigma = \sqrt{0.05}$ *(small jump component)*								
30	−0.03953	−0.0395	−0.0435	0.0000	0.00954	0.00955	0.01075	0.00001
35	−0.1430	−0.1431	−0.165	0.0000	0.02525	0.02528	0.03078	0.00003
40	−0.3193	−0.3194	−0.3948	−0.0001	0.03995	0.04001	0.05604	0.00006
45	−0.5228	−0.5229	−0.7143	−0.0001	0.04453	0.04455	0.07983	0.00002
50	−0.7014	−0.7016	−1	−0.0002	0.03879	0.03880	0	0.00001
Panel B. $\lambda = 5$, $\gamma = 0$, $\delta = \sqrt{0.05}$, *and* $\sigma = \sqrt{0.05}$ *(equal jump and smooth volatility)*								
30	−0.1645	−0.1648	−0.1744	−0.0003	0.01166	0.01170	0.01255	0.00004
35	−0.2474	−0.2478	−0.2654	−0.0004	0.01521	0.01524	0.01674	0.00003
40	−0.3357	−0.3361	−0.3644	−0.0004	0.01772	0.01774	0.02004	0.00002
45	−0.4227	−0.4230	−0.4656	−0.0003	0.01901	0.01901	0.02237	0.00000
50	−0.5035	−0.5038	−0.5626	−0.0003	0.01920	0.01920	0.02339	0.00009
Panel C. $\lambda = 5$, $\gamma = 0$, $\delta = 0.3$, *and* $\sigma = 0.10$ *(large relative jump volatility)*								
30	−0.1786	−0.1749	−0.1892	0.0037	0.01014	0.01134	0.01214	0.00120
35	−0.2489	−0.2551	−0.2759	−0.0061	0.01263	0.01134	0.01199	−0.00129
40	−0.3221	−0.3155	−0.3467	0.0067	0.01478	0.01464	0.01677	−0.00014
45	−0.3950	−0.4008	−0.4443	−0.0058	0.01594	0.01870	0.02014	0.00276
50	−0.4623	−0.4647	−0.5155	−0.0024	0.01590	0.01210	0.01431	−0.00380
Panel D. $\lambda = 5$, $\gamma = 0$, $\delta = \sqrt{0.05}$, *and* $\sigma = 0.05$ *(larger relative jump volatility)*								
30	−0.1511	−0.1588	−0.1719	−0.0077	0.01194	0.00508	0.00661	−0.00686
35	−0.2385	−0.2478	−0.2714	−0.0093	0.01641	0.02855	0.02822	0.01214
40	−0.3357	−0.3186	−0.3634	0.0171	0.02001	0.01087	0.01743	−0.00914
45	−0.4373	−0.4588	−0.5100	−0.0215	0.02219	0.02983	0.02981	0.007641
50	−0.5284	−0.5123	−0.6010	0.0160	0.02110	0.00983	0.02653	−0.01128

Put option Greeks on spot contracts. Merton is the benchmark for European puts. Numerical Greeks are from a (two) × seven-node tree. "A" denotes an American option and "E" denotes an European option. Error (E) is computed as the value of the seven-node European Greek minus the Merton Greek. The underlying pays no dividends and the spot price is $40. The risk-free rate is 8% and the option expires in one year. Relative jump volatility is defined as δ/σ. Computed from a 600-step tree.

The advantage of the bivariate tree is that we can use it to compute numerical partials for options with early exercise conditions, including those in real options. As Table 3 notes, there are important differences in European deltas and American deltas and, as expected, the differences increase monotonically with moneyness.

V. Real Options Example

The importance of the jump-diffusion tree extends beyond that of pricing American puts and calls. Specifically, the tree allows the use of backward solution techniques and thus the evaluation of complex derivatives and real options where value maximizing decisions are endogenous. The computations for a path-independent project are straightforward.

We demonstrate the pedagogy by using a five-node tree to value a project at time-n that imbeds an option to expand production. The underlying project net of options follows a jump-diffusion process, V. Project value, inclusive of future options but net of the expansion option, is given by P_n. The expansion option

https://doi.org/10.1017/S0022109000001915 Published online by Cambridge University Press

at time-n costs \$30 and adds value equal to $0.5V_n$. Thus, including all options, project value at time-n is given by

$$P_n^* = P_n + \text{Max}\{0.5V_n - 30, 0\}. \tag{21}$$

Values of the underlying are mapped onto the tree according to

$$V_n^{\pm}(j) = V_{n-1}e^{\pm\sigma\sqrt{\Delta}+(j-3)h}, \quad j = 1, 2, \ldots, 5. \tag{22}$$

Smooth probabilities are computed by equation (8) and probabilities at the five jump nodes are computed by equation (11). The values of the project exclusive of the expansion option are chosen exogenously. In an actual application, they would be endogenous and determined from terminal and interim boundary conditions. Parameter values and computations are given in Table 4. Note that the expansion option adds values in all states except when the smooth component is in the down state and the jump component is in its smallest state ($V_n^-(1) = \$52.64$). In this case, $P_n^{*-}(1) = P_n^-(1) = \$55$. The expansion adds greatest value at $V_n^+(5)$, where $0.5V_n^+(5) - \$130 = \$30.08$ is added. The continuation value at the previous node is

$$P_{n-1} = \frac{\sum_{j=1}^{5} pq_j P_n^{*+}(j) + \sum_{j=1}^{5}(1-p)q_j P_n^{*-}(j)}{1.025} = 98.22. \tag{23}$$

TABLE 4

Node Values and Probabilities: Two × Five-Node Tree

Diffusion Nodes	Jump Nodes				
	$-2h$	$-h$	0	h	$2h$
$V_n^{\pm}(j)$					
Up	62.82	74.10	87.39	103.08	121.58
Down	52.64	62.09	73.23	86.38	101.88
$P_n^{\pm}(j)$					
Up	70	80	95	110	130
Down	55	65	80	95	110
$P_n^{*\pm}(j)$					
Up	71.41	87.05	108.70	131.54	160.08
Down	55.00	66.05	86.62	108.18	130.94
	q_1	q_2	q_3	q_4	q_5
	0.01 305 9	0.04 290 5	0.940 9	0.002 559 8	0.0005 749 6
Probabilities					
$p = 0.69525$	0.0090793	0.029830	0.65416	0.0017797	0.00039974
$1 - p = 0.30475$	0.0039797	0.013075	0.28674	0.00078010	0.00017522

$P_n^* = P_n + \text{Max}(0.5V_n - 30, 0)$. Values of P_n are exogenous. Jump-diffusion parameters are: $\sigma = 0.125$, $\delta = 0$, $\gamma = -0.80$, $\gamma' = \gamma - \delta^2/2$, $\lambda = 0.10$, $r = 0.05$, $d = 0$, $\Delta = 0.5$, $h = \sqrt{(\gamma')^2 + \delta^2}$, and $V_{n-1} = 80$. The notation $V^+(j)$ refers to the value at the up-node in the smooth dimension and j-node in the jump dimension. Other values are similarly defined. Small p is the smooth diffusion up jump probability and q_j is the node j probability in the jump dimension.

Trigeorgis (1993) develops an expanded version of the above example with a 15-year project embedded with options to defer, abandon, abandon for salvage,

https://doi.org/10.1017/S0022109000001915 Published online by Cambridge University Press

https://doi.org/10.1017/S0022109000001915 Published online by Cambridge University Press

contract, and expand. Trigeorgis uses a smooth diffusion to represent the value of the project net of options. He then looks at the value of each option in isolation as well as the value of the collections of options. A significant feature of his example is that project options have interaction effects. Therefore, the portfolio value of options is not the sum of the value of individual options.

We evaluate the same project under the assumption that the process underlying project value net of options is a jump-diffusion. To highlight differences in option value, we also assume that the underlying process is subject to catastrophic changes of a magnitude of 80%. For example, a project involving a promising new drug could be denied approval by the FDA. Untimely deaths or other less drastic but damaging side effects after approval could also result in catastrophic loss of value. Schwartz and Moon (2000) consider in detail a drug project subject to a series of clinical trials. They permit the possibility of a catastrophic event that causes the project value to drop to zero with the probability governed by a Poisson counter.

Jump-diffusion parameters are normalized so that the initial value and variance of the process matches that of the smooth diffusion. Thus, the process differs only in the higher moments. Following Trigeorgis, the project setup is defined as follows:

i) Project value net of options[5] is denoted by V. The initial value is $V_0 = \$100$. The project has a nominal life of $T = 15$ years and an initial investment of \$10 is required.

ii) There is an option to abandon at the end of year two. If the project is abandoned, an outlay of \$90 is saved, giving project value $P^* = \text{Max}(P - 90, 0)$.

iii) An investment of \$35 is required in year five. However, the project may be contracted by 25% in year five for an outlay of only \$10, saving \$25. The project value is $P^* = P + \text{Max}(25 - 0.25V, 0)$, where V is project value net of options.

iv) The project may be expanded by 50% in year seven by investing \$30. The project value is then $P^* = P + \text{Max}(0.5V - 30, 0)$.

v) There is a salvage option at any time worth $\text{Max}(0.5S, 0)$, where S is the value of invested cash flows attenuated by a 10% decay per year.

Table 5 compares real option values under a jump-diffusion process with those from a smooth diffusion. Both processes are parameterized to have the same process mean and volatility. The jump-diffusion process parameters are set to mimic a relatively rare but catastrophic event. The intensity parameter $\lambda = 0.10$ implies an average of one jump per 10 years. The jump magnitude is fixed at $\gamma = -0.8$ corresponding to an 80% loss of net project value. These parameters and smooth volatility = 0.125 give a process volatility of 0.2822. The interest rate is fixed at 0.05.

The jump-diffusion options, taken in isolation, are less valuable than those suggested by geometric Brownian motion. Percentage differences $(((jd - gbm)/gbm) \times 100)$ for options taken in isolation are: -19.87 (abandon), -10.96 (con-

[5]Trigeorgis refers to project value net of options as gross project value.

TABLE 5

Value of Project Options

Options	Option Values		Difference (%)
	Smooth Diffusion (*gbm*)	Jump Diffusion (*jd*)	$\frac{jd - gbm}{gbm} \times 100$
A	22.23	17.81	– 19.87
C	3.146	2.801	– 10.96
E	30.28	30.27	– 0.027
S	24.61	19.92	– 19.06
AC	22.40	20.23	– 18.60
AE	45.28	43.52	– 3.886
AS	24.61	19.92	– 19.06
CE	33.43	33.08	– 1.056
CS	24.72	20.25	– 18.09
ES	46.89	44.87	– 4.306
ACE	45.78	44.25	– 3.342
ACS	24.72	20.25	– 18.09
CES	47.38	45.50	– 3.964
ACES	47.38	45.50	– 3.964

Option values obtained from a 900-step bivariate tree. Parameters are $r = 0.05$, $\sigma = 0.125$, $\lambda = 0.10$, $\gamma = -0.80$, and $\delta = 0$. Total process volatility is 0.2822. Initial gross project value is $V_0 = 100$ and the project's nominal life is 15 years. $A \Rightarrow$ abandon option at year 2, $C \Rightarrow$ contract option at year 5, $E \Rightarrow$ expand option at year 7 and S is the option to abandon the project for salvage at any time. See Trigeorgis (1993) for additional details on the project setup.

tract), −0.02685 (expand), and −19.06 (salvage). Figure 3 can explain these results, where Graph A is the probability density function for jump-diffusion and geometric Brownian motion densities at time $T = 3$.[6] The value of the *abandonment* option is the conditional expected value of the payoffs to the left of the critical point. Notice that the geometric Brownian motion probability mass is greater than that of the jump-diffusion in this region. The geometric Brownian motion abandonment option has greater value than the jump-diffusion abandonment option. Similarly, the *contract* option depends on the probability density function at $T = 5$. To the left of the critical point, the probability mass of geometric Brownian motion is greater than that of jump-diffusion at almost every point (Graph B). The result is that the geometric Brownian motion contract option value exceeds that of the corresponding jump-diffusion. The density at $T = 7$ is more ambiguous with respect to the critical point and, in fact, the distributions produce almost identical option values for projection *expansion* (Figure 3, Graph C).

For short horizons, the jump-diffusion process produces peaks in the probability density function corresponding to the number of jumps. This is especially noticeable when jump magnitude (γ) is large relative to jump volatility (δ). For example, an examination of conditional probabilities shows that the peak in Figure 3, Graph A at $V = 130$ corresponds to zero jumps while the peak at $V = 60$ corresponds to one jump. For longer horizons, the jump component is attenuated by the smooth component as Figure 3, Graph D shows. Graph D also shows that, long-term, jump-diffusions have fat tails relative to geometric Brownian motion.

[6]The conditional distribution of $f(S|n)$ is lognormal and $f(n)$ is Poisson. The jump-diffusion probability density, $f(S)$, is obtained by computing $f(S|n)f(n) = f(S, n)$ and $f(S) = \sum_n f(S, n)$.

https://doi.org/10.1017/S0022109000001915 Published online by Cambridge University Press

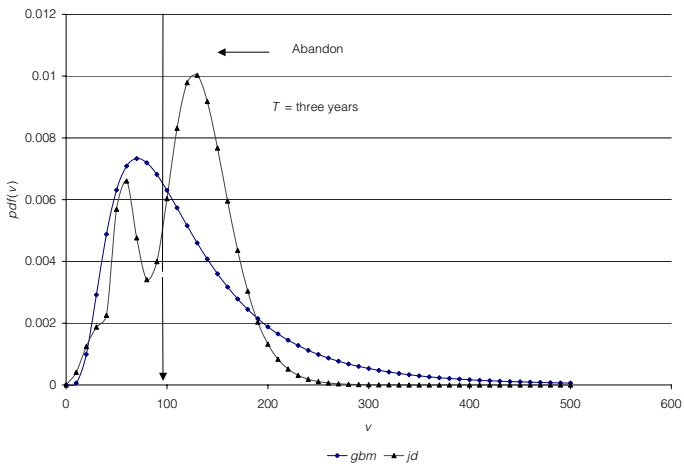
VI. Conclusions

The standard jump-diffusion process is mapped onto a two-factor bivariate tree. The first factor is a discrete version of the smooth diffusion process and the second factor simulates log-normal jumps under Poisson compounding. We

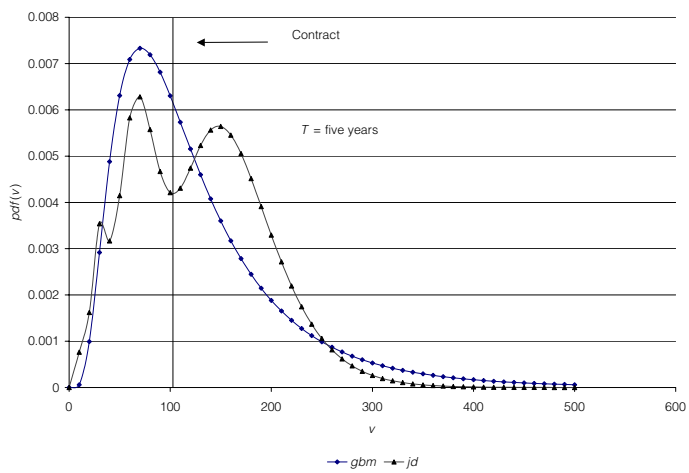
FIGURE 3

Probability Density Function (three-, five-, seven-, and 15-year intervals)

Graph A. Probability Density Function at Three Years



Graph B. Probability Density Function at Five Years

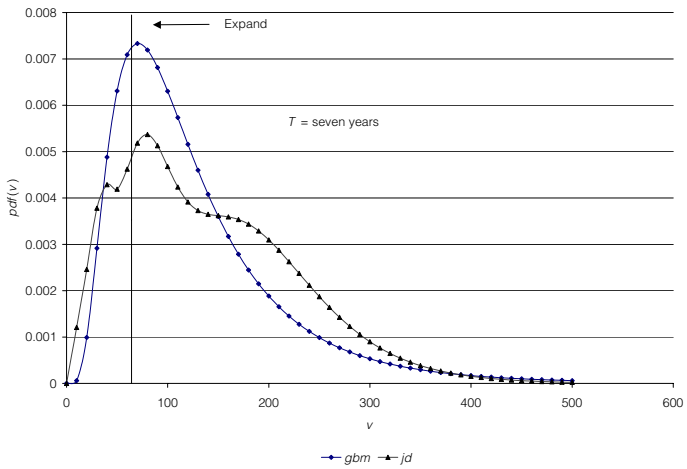


https://doi.org/10.1017/S0022109000001915 Published online by Cambridge University Press

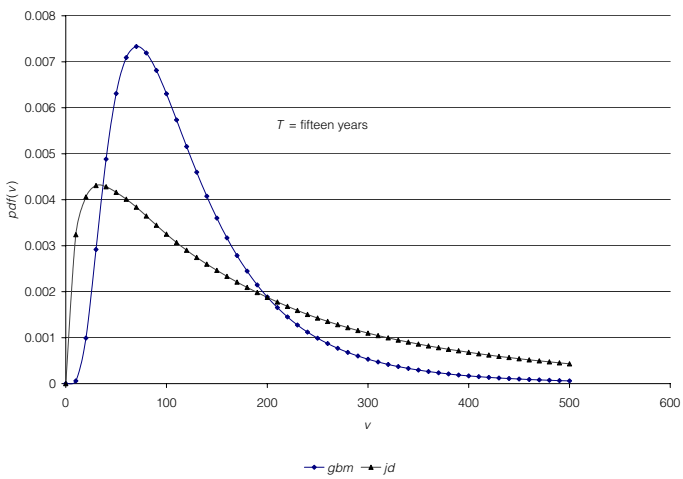
FIGURE 3 (continued)

Probability Density Function (three-, five-, seven-, and 15-year intervals)

Graph C. Probability Density Function at Seven Years



Graph D. Probability Density Function at 15 Years



Parameters are $\lambda = 0.10$, $\sigma = 0.125$, $\gamma = -0.80$, $\delta = 0$, $r = 0.05$, and $V_0 = \$100$.

investigate jumps in the second factor to five-, seven-, and nine-nodes, matching the first four, six, and eight local moments, respectively. For the options evaluated in this paper, the seven-node algorithm is slightly more accurate than the five-node version and generally matches the accuracy of the nine-node algorithm. Weak convergence obtains at arbitrary but finite time T for fixed jumps while otherwise convergence is obtained for the first $M - 1$ cumulants in an M-node tree. Because of the flexibility of the tree approach to pricing, the methodology is uniquely

https://doi.org/10.1017/S0022109000001915 Published online by Cambridge University Press

useful for evaluating non-path-dependent American options and real options with non-standard payoff functions. The bivariate algorithm is straightforward and easy to implement.

Appendix A. Inverting the Moment Matrix

The moment matrix is a Vandermonde matrix (Press, Taulkolsky, Vetterling, and Flannery (1992)). The inverse of this matrix can be obtained exactly by identifying appropriate coefficients in Lagrange interpolating polynomials up to order $2m + 1$, where $2m$ is the number of moments to be matched. The polynomials are

$$P_j(x) = \prod_{n=1}^{2m+1} \frac{(x - x_n)}{x_j - x_n}, \quad j = 1, 2, \ldots, 2m + 1, \tag{A-1}$$

where terms corresponding to $x - x_j$ are omitted from the numerator and the term $x_j - x_j$ is omitted from the denominator. The x_n are the elements corresponding to the elements of the A matrix found in row 2 with the element in column j omitted. For seven-node, these elements are, respectively, $-2, -1, 0, 1, 2, 3$ for P_1, $-3, -1, 0, 1, 2, 3$ for P_2, and so on. The inverse may be obtained by expressing the polynomials in matrix form. The matrix formulation of the first seven Lagrangian polynomials is:

$$\begin{pmatrix} P_1(x) \\ P_2(x) \\ P_3(x) \\ P_4(x) \\ P_5(x) \\ P_6(x) \\ P_7(x) \end{pmatrix} = \frac{1}{6!} \begin{pmatrix} 0 & -12 & 4 & 15 & -5 & -3 & 1 \\ 0 & 108 & -54 & -120 & 60 & 12 & -6 \\ 0 & -540 & 540 & 195 & -195 & -15 & 15 \\ 720 & 0 & -980 & 0 & 280 & 0 & -20 \\ 0 & 540 & 540 & -195 & -195 & 15 & 15 \\ 0 & -108 & -54 & 120 & 60 & -12 & -6 \\ 0 & 12 & 4 & -15 & -5 & 3 & 1 \end{pmatrix} \begin{pmatrix} 1 \\ x \\ x^2 \\ x^3 \\ x^4 \\ x^5 \\ x^6 \end{pmatrix}. \tag{A-2}$$

The coefficient matrix on the right-hand side is A^{-1}, the inverse of the moment matrix for a seven-node tree.

Appendix B. Cumulants and Moments

The cumulants of the jump process under Poisson compounding follow directly from the characteristic function in equation (14):

$$\begin{aligned}
\kappa_1 &= \lambda\Delta(\gamma') \\
\kappa_2 &= \lambda\Delta((\gamma')^2 + \delta^2) \\
\kappa_3 &= \lambda\Delta((\gamma')^3 + 3(\gamma')\delta^2) \\
\kappa_4 &= \lambda\Delta((\gamma')^4 + 6\delta^2(\gamma')^2 + 3\delta^4) \\
\kappa_5 &= \lambda\Delta((\gamma')^5 + 10\delta^2(\gamma')^3 + 15\delta^4(\gamma')) \\
\kappa_6 &= \lambda\Delta((\gamma')^6 + 15\delta^2(\gamma')^4 + 45\delta^4(\gamma')^2 + 15\delta^6) \\
\kappa_7 &= \lambda\Delta((\gamma')^7 + 21\delta^2(\gamma')^5 + 105\delta^4(\gamma')^3 + 105\delta^6(\gamma')) \\
\kappa_8 &= \lambda\Delta((\gamma')^8 + 28\delta^2(\gamma')^6 + 210\delta^4(\gamma')^4 + 420\delta^6(\gamma')^2 + 105\delta^8).
\end{aligned}$$

Moment-cumulant relations are given in Stuart and Ord (1994).

https://doi.org/10.1017/S0022109000001915 Published online by Cambridge University Press

Appendix C. Order of Convergence

As in Leisen (1998), the order of convergence is defined as ρ, where the absolute value of the approximation error is

$$\epsilon = \beta n^{-\rho}, \tag{C-1}$$

and n is the number of steps in the tree. Thus, the log of absolute errors should be linear in $\log(n)$ and have slope $-\rho$. From equation (C-1), note that an approximation of order ρ implies that the error is $O(1/n^{\rho})$. Leisen (1998) shows that the Cox, Ross, and Rubenstein (1979) binomial model converges with order one. Furthermore, a number of extensions of the binomial model, including those of Jarrow and Rudd ((1983), p. 188) and Tian (1997) are also of order one.

Figure 2 demonstrates order one convergence for the seven-node jump-diffusion approximation. Parameters for the in-the-money European call option simulated are: $\sigma = 0.20$, $\lambda = 10$, $\gamma = 0.01$, $\delta = 0.03$, $r = 1.10$, and $T = 0.25$. The futures underlying is \$250 and the strike is \$235. A straight line of slope -1 corresponding to order one convergence is imposed on the graph to facilitate comparison. Just below the line, absolute errors are plotted vs. $\log(n)$, the result being an almost identical slope of -1.[7] To quantify the order of convergence, a log regression is fitted to equation (C-1). The slope coefficient is $\hat{\rho} = -0.98$ and the coefficient of determination is $R^2 = 0.99$.

At-the-money and out-of-the-money calls are also evaluated. The slopes are, respectively, 0.936 and 0.919 with R^2s of 0.74 and 0.75. Thus, the order of convergence for these cases is approximately one and equivalent to that of the one-factor binomial. However, the number of steps is mapped into a bivariate state space so the M-node algorithm at step n requires a plane of $(n+1)[M + (M-1)(n-1)]$-nodes that is $O(n^2)$ compared to a plane that is $O(n)$ for the one-factor binomial. We time the seven-node algorithm using a Fortran compiler and an Athlon 2400 Mhz processor. It takes about one second to price a 150-step tree and about 10 seconds to price a 300-step tree. Execution time is approximately log-linear in steps and is given by $6e^{-18.42}\, n^{3.32}$ seconds.

References

Amin, K. "Jump Diffusion Valuation in Continuous Time." *Journal of Finance*, 48 (1993), 1833–1863.

Bakshi, G.; C. Cao; and Z. Chen. "Empirical Performance of Alternative Option Pricing Models." *Journal of Finance*, 52 (1997), 2003–2049.

Bakshi, G., and Z. Chen. "An Alternative Valuation Model for Contingent Claims." *Journal of Financial Economics*, 44 (1997), 123–165.

Bakshi, G., and C. Cao. "Disentangling the Contribution of Return-Jumps and Volatility-Jumps: Insights from Individual Equity Options." Unpubl. Working Paper, Univ. of Maryland (2004).

Ball, C. A., and W. N. Torous. "On Jumps in Common Stock Prices and Their Impact on Call Option Pricing." *Journal of Finance*, 40, (1985), 155–173.

Barone-Adesi, G., and R. E. Whaley. "Efficient Analytic Approximation of American Option Values." *Journal of Finance*, 42 (1987), 301–320.

Bates, D. S. "The Crash of '87: Was it Expected? The Evidence from Options Markets." *Journal of Finance*, 46 (1991), 1009–1044.

Bates, D. S. "Jumps and Stochastic Volatility: Exchange Rate Processes Implicit in Deutsche Mark Options." *Review of Financial Studies*, 9 (1996), 69–107.

Black, F., and M. Scholes. "The Pricing of Options and Corporate Liabilities." *Journal of Political Economy*, 8 (1973), 637–659.

Cox, J. C.; S. A. Ross; and M. Rubenstein. "Option Pricing: A Simplified Approach." *Journal of Financial Economics*, 7 (1979), 229–263.

[7] Equally spaced points, n_j on the log scale starting at 10 were chosen according to $n_j = \text{Int}(10^{1+.04j})$, $j = 0, 1, 2, \ldots$.

https://doi.org/10.1017/S0022109000001915 Published online by Cambridge University Press

Das, S. R., and R. K. Sundaram. "Of Smiles and Smirks: A Term Structure Perspective." *Journal of Financial and Quantitative Analysis*, 34 (1999), 211–240.
Duffie, D.; J. Pan; and K. Singleton. "Transform Analysis and Asset Pricing for Affine Jump-Diffusions." *Econometrica*, 68 (2000),1343–1376.
Eraker, B. "Do Stock Prices and Volatility Jump? Reconciling Evidence from Spot and Option Prices." *Journal of Finance*, 50 (2004), 1367–1403.
Jarrow, R., and A. Rudd. *Option Pricing*. Homewood, IL: Irwin (1983), 183–188.
Jorion, P. "On Jump Processes in the Foreign Exchange and Stock Markets." *Review of Financial Studies*, 1 (1988), 427–445.
Kushner, H., and G. DiMasi. "Approximations for Functionals and Optimal Control on Jump Diffusion Processes." *Journal of Mathematical Analysis and Applications*, 40 (1978), 772–800.
Leisen, D. "Pricing the American Put Option: A Detailed Convergence Analysis for Binomial Models." *Journal of Economic Dynamics and Control*, 22 (1998), 1419–1444.
MacMillan, L. W. "Analytic Approximation for the American Put Option." *Advances in Futures and Options Research*, 1 (1987), 119–139.
Merton, R. C. "Option Pricing When Underlying Stock Returns Are Discontinuous." *Journal of Financial Economics*, 3 (1976), 125–144.
Naik, V., and M. Lee. "General Equilibrium Pricing of Options on the Market Portfolio with Discontinuous Returns." *Review of Financial Studies*, 3 (1990), 493–521.
Nelson, D. B., and K. Ramaswamy. "Simple Binomial Processes as Diffusion Approximations in Financial Models." *Review of Financial Studies*, 3 (1990), 393–430.
Pan, J. "The Jump-Risk Premia Implicit in Options: Evidence from an Integrated Time-Series Study." *Journal of Financial Economics*, 63 (2002), 3–50.
Press, W. H.; S. Taulkolsky; W. Vetterling; and B. Flannery. *Numerical Recipes in C: The Art of Scientific Computing*, 2nd ed. Cambridge, England: Cambridge Univ. Press (1992).
Schwartz, E. S., and M. Moon. "Evaluating Research and Development Investments." In *Project Flexibility, Agency and Competition: New Developments in the Theory and Applications of Real Options*, M. Brennan and L. Trigeorgis, eds. New York, NY: Oxford Univ. Press (2000).
Stuart, A., and K. Ord. *Kendall's Advanced Theory of Statistics: Vol. 1*. New York, NY: Oxford Univ. Press (1994).
Tian, Y. "A Modified Lattice Approach to Option Pricing." *Journal of Futures Markets*, 13 (1993), 563–577.
Trigeorgis, L. "A Log-Transformed Binomial Numerical Analysis Method for Valuing Complex Multi-Option Investments." *Journal of Financial and Quantitative Analysis*, 26 (1991), 309–326.

https://doi.org/10.1017/S0022109000001915 Published online by Cambridge University Press